

# UC Riverside

## UC Riverside Previously Published Works

### Title

Fullerene–Porphyrin Constructs

### Permalink

<https://escholarship.org/uc/item/36c0038t>

### Journal

Accounts of Chemical Research, 38(4)

### ISSN

0001-4842

### Authors

Boyd, Peter DW  
Reed, Christopher A

### Publication Date

2005-04-01

### DOI

10.1021/ar040168f

Peer reviewed

# Fullerene—Porphyrin Constructs

PETER D. W. BOYD\*

Department of Chemistry, The University of Auckland,  
Private Bag 92019, Auckland, New Zealand

CHRISTOPHER A. REED\*

Department of Chemistry, University of California,  
Riverside, California 92521-0403

Received June 17, 2004

## ABSTRACT

Porphyrins and fullerenes are spontaneously attracted to each other. This new supramolecular recognition element can be used to construct discrete host–guest complexes, as well as ordered arrays of interleaved porphyrins and fullerenes. The fullerene–porphyrin interaction underlies successful chromatographic separations of fullerenes, and there are promising applications in the areas of porous framework solids and photovoltaic devices.

## Introduction

The manipulation of weak forces to construct new molecular architectures is a major theme of contemporary chemistry. Traditionally, H-bonding, electrostatics, labile metal–ligand bonds, and flat  $\pi$ – $\pi$  interactions have been used to assemble new structures. This Account concerns a newly recognized supramolecular recognition element: the attraction of the curved  $\pi$  surface of a fullerene to the center of the flat  $\pi$  surface of a porphyrin or metalloporphyrin. The traditional paradigm of supramolecular chemistry is not followed inasmuch as it is not necessary to match a concave host with a complementary convex guest.<sup>1</sup>

The close association of a fullerene and a porphyrin was first recognized in the molecular packing of a crystal structure containing a covalent fullerene–porphyrin conjugate, **1** (Figure 1).<sup>2</sup> The 2.75 Å approach of a fullerene carbon atom to the center of the neighboring porphyrin plane was notably shorter than the separations of familiar  $\pi$ – $\pi$  interactions. Graphite and typical arene/arene separations are in the range 3.3–3.5 Å. Interfacial porphyrin–porphyrin separations are  $>3.2$  Å,<sup>3,4</sup> fullerene–arene

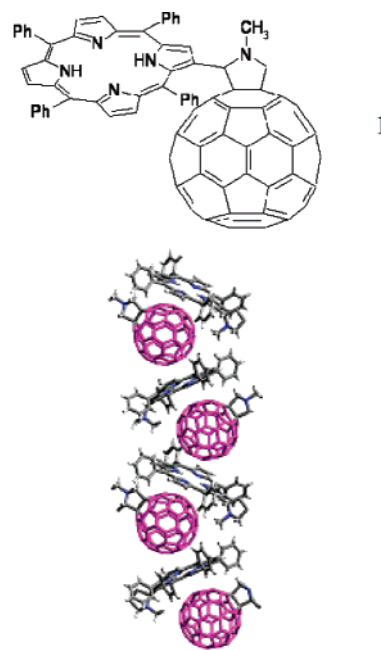


**FIGURE 1.** The close approach of a fullerene to the center of a porphyrin in the crystal structure of **1**.

approaches lie in the range 3.0–3.5 Å,<sup>1</sup> and fullerene–fullerene separations are typically ca. 3.2 Å. A precedent for the close approach of a fullerene to a porphyrin can be found in the structure of a C<sub>60</sub> complex of a nickel porphyrazine reported in 1995.<sup>5</sup>

The fullerene–porphyrin association was proposed to be attractive and structure-defining. In addition to a  $\pi$ – $\pi$  attraction, the centering was viewed as the result of an interaction between the electron density of a 6:6 ring juncture of the fullerene (i.e., the “double” bond) and the electropositive center of the porphyrin. The extent of charge transfer, if any, and its direction have become a matter of debate.

## Fullerene—Porphyrin and Fullerene—Metalloporphyrin Cocrystallates

The generality of the fullerene–porphyrin attraction quickly became apparent in work with tetraphenylporphyrins from our labs<sup>6</sup> and with metalloctaethylporphyrins in the labs of Balch & Olmstead.<sup>7</sup> Almost any free-base porphyrin or metalloporphyrin (or like macrocycle) can be cocrystallized with almost any fullerene (or derivatized fullerene) from comixed solutions.<sup>8–13</sup>

Representative examples are illustrated by H<sub>2</sub>TPP·C<sub>60</sub>·3toluene (H<sub>2</sub>TPP = tetraphenylporphyrin) and 2Co(OEP)·C<sub>60</sub>·CHCl<sub>3</sub> (OEP = dianion of octaethylporphyrin). As shown in Figures 2 and 3, the structures often adopt an alternating zigzag motif. The less sterically hindered OEP complexes usually retain the face-to-face porphyrin–porphyrin motif commonly seen in structures of the parent porphyrins. A minority of structures have fullerene–fullerene contacts. This suggests that, in the absence of steric effects, the hierarchy of interaction strengths is

Peter D. W. Boyd was born in Buckinghamshire, U.K., in 1946. He received his B.Sc. from the University of Tasmania and Ph.D. from Monash University. After postdoctoral studies at the University Chemical Laboratory, Cambridge, he was awarded a Queen Elizabeth Fellowship to work at the Research School of Chemistry, Australian National University. He joined the Chemistry Department of The University of Auckland in 1978 and is currently an Associate Professor in Chemistry. His current research interests include the chemistry of porphyrins and fullerenes, their supramolecular assembly, and computational studies of the electronic structure and properties of molecules.

Christopher A. Reed was born in New Zealand in 1947 and educated at The University of Auckland. After postdoctoral studies at Stanford University, he joined the faculty at the University of Southern California in 1973. In 1998, he moved to the University of California, Riverside, as Distinguished Professor. He has been awarded Sloan, Dreyfus Teacher–Scholar, Guggenheim, and von Humboldt Fellowships. His current research interests include the chemistry of iron porphyrins, magnetochemical phenomena, framework solids, fullerenes, carborene anions, superacids, carbocations, and reactive cations across the periodic table.

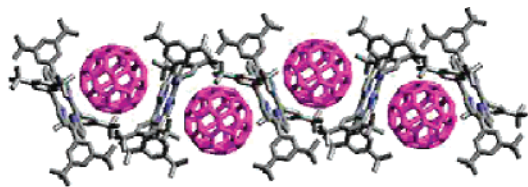


**FIGURE 2.** Zigzag alternating  $C_{60}$  and  $H_2TPP$  moieties in  $H_2T_{3,5}\text{-di-}t\text{-butylPP}\cdot C_{60}$ .<sup>6</sup> Solvate molecules have been omitted for clarity.

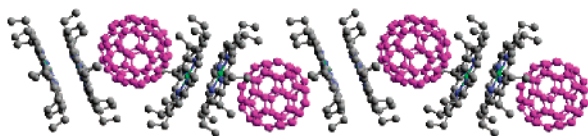


**FIGURE 3.** Zigzag alternating  $C_{60}$  and  $\{Co(OEP)\}_2$  moieties in  $2Co(OEP)\cdot C_{60}\cdot CHCl_3$ .<sup>7</sup> The solvate molecule has been omitted for clarity.

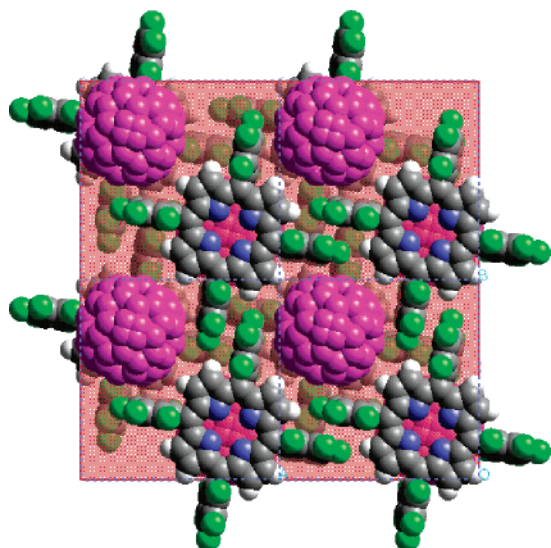


**FIGURE 4.** Structure of  $H_2TPFP\cdot C_{60}$  showing alignment of porphyrin sheets formed with  $C_6F_5(C-F)\cdots(H-C)$  porphyrin interactions (green).<sup>17</sup>

porphyrin–porphyrin > porphyrin–fullerene > fullerene–fullerene. Some porphyrins depart significantly from planarity. They can be domed, ruffled, or warped in a variety of ways for a variety of reasons. This can have the effect of partially wrapping a fullerene,<sup>12,14</sup> presumably enhancing the  $\pi$ – $\pi$  interactions.

To date there have been no reports of phthalocyanine–fullerene cocrystallates, although scanning tunneling microscopy (STM) imaging of  $Cu(\text{phthalocyanine})$ <sup>15</sup> and  $B(\text{subphthalocyanine})$ <sup>16</sup> on a close-packed  $C_{60}$  film has been investigated.

The fullerene–porphyrin “embrace” can steer the development of further crystal organization by cooperating with other supramolecular recognition and crystal packing elements. An informative example is provided by the cocrystallate  $H_2TPFP\cdot C_{60}$  ( $H_2TPFP$  = tetra(pentafluorophenyl)porphyrin), which, as shown in Figure 4, combines the strict tetragonal register of alternating fullerenes and porphyrins with 2D sheets connected by (pentafluorophenyl)porphyrin  $C-F\cdots H-C$  hydrogen bridge interactions.<sup>17</sup> Although this structure postdated the fullerene-pillared sheet structures discussed below, it illustrates the

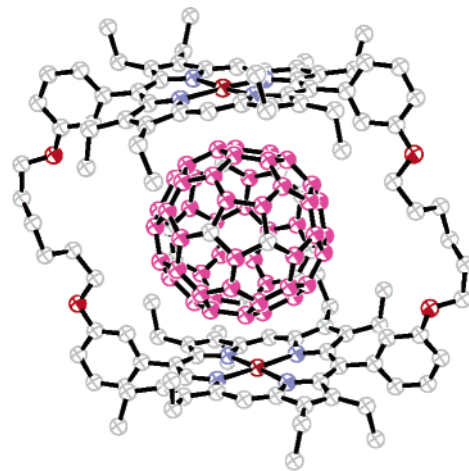


**FIGURE 5.** X-ray structure of  $C_{60}$  bound to a cyclic bisporphyrin host.<sup>19</sup>

developing concept of engineering extended framework solids using the fullerene–porphyrin molecular attraction as a primary organizational element.

### Host–Guest Complexation

The fullerene–porphyrin interaction observed in cocrystallates is not merely a feature of the solid state; it persists in solution. Small but significant mutual upfield ring current-induced shifts were detected in the  $^1H$  NMR spectrum of the  $H_2TPP$  and the  $^{13}C$  NMR spectrum of  $C_{60}$  of mixtures in toluene solution.<sup>6</sup> Discrete 1:1 complexes with high binding constants for  $C_{60}$  and  $C_{70}$  were obtained by constructing hosts having two porphyrins about 12 Å apart. This creates a good fit for  $C_{60}$  and  $C_{70}$  since they have van der Waals diameters of about 10 Å. Cyclic bisporphyrins were first designed by Aida, Tashiro and co-workers<sup>18,19</sup> and acyclic (“Jaws”) bisporphyrins were first designed in our labs.<sup>14,20</sup> These are illustrated in the crystal structure of a  $C_{60}$  adduct in Figure 5 and the crystal structure of a  $C_{70}$  adduct in Figure 6. The egg-shaped  $C_{70}$  binds with the equatorial belt region closest to the porphyrin planes, a feature that had been previously deduced from its  $^{13}C$  NMR spectrum. As shown in Figure 7, the magnitudes of the upfield shifts of the five different types of C atoms (a to e) increase progressively from the pole to the belt region.<sup>20</sup> The binding of  $C_{70}$  at its equatorial region rather than the poles must be driven by the greater  $\pi$ – $\pi$  contact area available to the porphyrin from the less curved regions of the fullerene.<sup>6</sup>

The observation of mutual upfield ring current effects in fullerene–porphyrin complexes is a general phenomenon. It has even been observed in the solid state where rapid rotation of fullerenes allows the detection of sharp signals. The  $^{13}C$  cross-polarization magic angle spinning (CPMAS) NMR spectrum of the  $H_2TPP\cdot C_{60}\cdot 3\text{toluene}$  cocrystallate shows a 3.2 ppm upfield shift of the  $C_{60}$  signal relative to free  $C_{60}$  powder.<sup>14</sup>

More recent porphyrin hosts have employed a Pd-induced cleft,<sup>21</sup> a dendritic hexamer showing allosteric binding,<sup>22</sup> a tetramer showing negative cooperativity,<sup>23</sup> a calixarene-linked dimer,<sup>24</sup> a dendritically elaborated por-

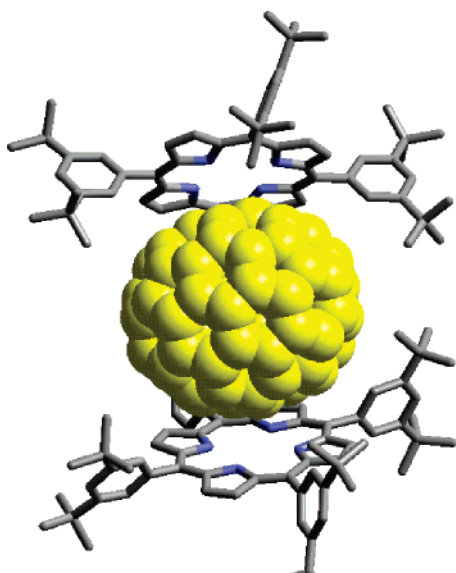


**FIGURE 6.** X-ray structure of  $C_{70}$  side-bound to a “Jaws porphyrin” host.<sup>14</sup>

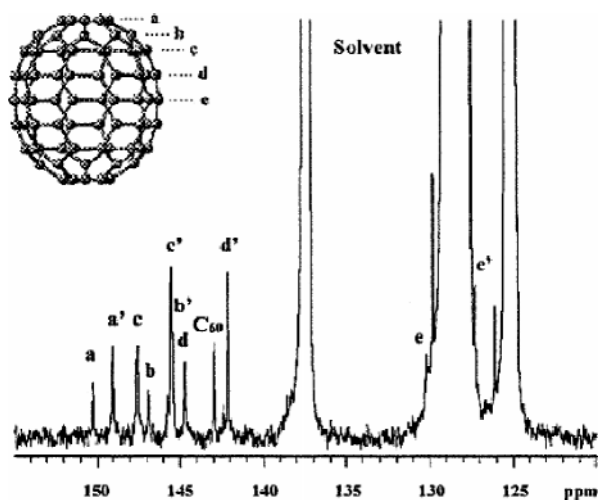


**FIGURE 7.** Low temperature ( $-60\text{ }^{\circ}\text{C}$ )  $^{13}\text{C}$  NMR spectrum of a toluene solution of 1.5:1 mixture of  $C_{70}$  and Jaws porphyrin. Resonances a–e arise from free  $C_{70}$  and a'–e' from complexed  $C_{70}$ .<sup>20</sup>

phyrin,<sup>25</sup> and a pentaporphyrin box.<sup>26</sup> The porphyrin–fullerene attraction has also been shown to be important in the assembly of gels<sup>27</sup> and augmenting other host–guest complexation.<sup>28</sup>

### The Nature of the Fullerene–Porphyrin Interaction

The experimental observations regarding the nature of the fullerene–porphyrin interaction can be summarized as follows.

In the vast majority of structures the 6:6 ring juncture bond of the fullerene, rather than the 6:5 ring juncture bond, lies closest to the porphyrin or metalloporphyrin plane. These 6:6 “double” bonds of fullerenes are more electron-rich than the 5:6 “single” bonds. They are centered over the electropositive center of the porphyrin or

metalloporphyrin with the closest  $C_{\text{fullerene}}$ -to-porphyrin plane distances of 2.6–3.0 Å.

Binding constant data for a variety of bisporphyrins are given in Tables 1 and 2. The binding of fullerenes to free-base porphyrin hosts is often of comparable strength to zinc porphyrins and somewhat surprisingly, stronger than a number of other first row transition metalloporphyrin hosts. This suggests that covalent metal–ligand bonding is not of major importance, at least for first row metals. A Rh(III) porphyrin shows higher affinity, attributable to more significant M–C metal–ligand bonding for a second row metal.

Typically, the metal in a metalloporphyrin–fullerene structure is not significantly drawn out of the plane toward the fullerene, although  $[\text{Fe}^{\text{III}}(\text{TPP})(\text{C}_{60})]^+$  is a notable exception.<sup>30</sup> Probably because of nonplanarity effects, the Cu atom in  $\text{Cu}_2(\text{JawsP})$  actually shows a small out-of-plane displacement (0.024 Å) away from the fullerene.

In an *N*-methylpyrrolidine-derivatized fullerene structure, the carbon atom closest to the porphyrin center is three atoms removed from the functionality. A semiempirical molecular orbital (MO) calculation shows this to be the most negative C atom that is sterically accessible to the porphyrin plane, suggesting an electrostatic component to the orientation of the fullerene.<sup>20</sup>

The complex of  $\text{Fe}(\text{TPP})^+$  with  $C_{60}$  is green rather than purple, the expected color of the combined unperturbed chromophores.<sup>6</sup> This implies charge transfer via coordinate bonding. The Fe atom is slightly out-of-plane (ca. 0.03 Å) toward the  $C_{60}$  indicating the presence of a weak axial coordinate bond (ca. 2.63 Å) with at least some degree of covalence. The Fe(III) center is cationic, and its  $d_z^2$  orbital is only half occupied, suggesting that the direction of charge transfer is with the fullerene as the donor. The likely orbital involvement was identified by density functional theory in closely related complexes of  $\text{Fe}(\text{TPP})^+$  with  $\eta^2$ -bonded arenes.<sup>30</sup>

$C_{60}^{1-}$  fullerides appear to bind to metalloporphyrins more strongly than  $C_{60}$  fullerenes.<sup>31</sup> The Co–C bond in  $[\text{Co}^{\text{II}}(\text{TPP})(\text{C}_{60})]^-$  is  $\sim 0.4$  Å shorter than that in  $\text{Co}^{\text{II}}(\text{TPP})\text{-C}_{60}$ , and the Co atom is displaced  $\sim 0.1$  Å from the mean porphyrin plane toward  $C_{60}$ . This is consistent with the notion of the fullerene moiety acting as the electron donor to the metalloporphyrin. Significant covalence in the metal–carbon bonding is indicated by the overall diamagnetism of  $[\text{Co}^{\text{II}}(\text{TPP})(\text{C}_{60})]^-$ . Both  $\text{Co}(\text{TPP})$  and  $C_{60}^{1-}$  lose the  $S = 1/2$  spin associated with their uncomplexed states. The bonding has not been analyzed in detail but conventional wisdom would suggest  $\sigma$  overlap of the Co  $d_z^2$  orbital with the delocalized  $\pi$  orbitals of the fullerene.

Small red shifts of the Soret (Q) bands in the absorption spectra of porphyrins and metalloporphyrins (up to 7 nm) are frequently seen upon complexation of fullerenes. This may reflect a small degree of charge transfer between the fullerene to the porphyrin ring, lowering the energy of the porphyrin  $\pi$  to  $\pi^*$  transition. Porphyrin fluorescence is quenched by the close approach of a fullerene, and this is generally observed. Porphyrin–fullerene films have been reported to exhibit an emission band at  $\sim 800$  nm.<sup>32</sup> This

**Table 1. Binding Constants ( $M^{-1}$ ) of Cyclic Porphyrin Dimer and JAWS Porphyrin**

host		H <sub>2</sub>	Zn	Mn	Fe	Co	Cu	Pd	Ag	Rh	ref
cyclic porphyrin dimer	C <sub>60</sub>	$7.94 \times 10^5$	$6.31 \times 10^5$			$2.00 \times 10^6$	$5.01 \times 10^5$		$1.26 \times 10^5$	$2.51 \times 10^7$	19
	C <sub>70</sub>	$1.58 \times 10^7$	$2.00 \times 10^7$			$1.26 \times 10^7$	$5.01 \times 10^6$		$3.16 \times 10^6$	$10^8$	19
	C <sub>120</sub>									$8.32 \times 10^6$	29
JAWS porphyrin	C <sub>60</sub>	$5.20 \times 10^3$	$1.95 \times 10^3$	$2.76 \times 10^3$	$4.90 \times 10^2$	$2.98 \times 10^3$	$4.86 \times 10^3$	$8.15 \times 10^2$			20

**Table 2. Binding Constants ( $M^{-1}$ ) of a Variety of Bisporphyrins**

host		H <sub>2</sub>	Zn	ref
Pd bisporphyrin cleft	C <sub>60</sub>		$3.7 \times 10^4$	21
dendritic porphyrin monomer	C <sub>60</sub>	$2.57 \times 10^4$		25
Zn(por)[RuPor] <sub>4</sub> box	C <sub>60</sub>		$9.65 \times 10^3$	26
terphenyl porphyrin tetramer	C <sub>60</sub> (1)	$5.8 \times 10^3$		23
terphenyl porphyrin tetramer	C <sub>60</sub> (2)	$2.00 \times 10^3$		23
dimer(2)	C <sub>60</sub>	154		23
dimer(3)	C <sub>60</sub>	566		23
porphyrin hexamer 1:3	C <sub>60</sub>		$1.4 \times 10^8$	22
calixarene bisporphyrin	C <sub>60</sub>	$4.92 \times 10^3$	$8.60 \times 10^3$	24
calixarene bisporphyrin	C <sub>70</sub>	$2.11 \times 10^4$	$2.80 \times 10^4$	24
thiacalixarene bisporphyrin	C <sub>60</sub>	$2.34 \times 10^3$	$2.71 \times 10^3$	24

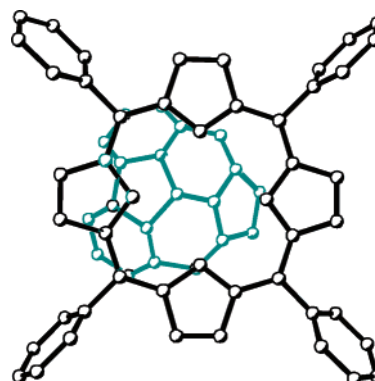
band is not seen in films of the separate chromophores or in solutions of the mixed components. It is therefore attributed to a charge transfer state arising from the fullerene–porphyrin interaction. NIR absorption bands attributed to porphyrin-to-fullerene charge-transfer bands have been observed in solid spectra of porphyrin–fullerene cocrystallates.<sup>12</sup>

Near-edge X-ray absorption fine structure (NEXAFS) measurements on a Zn porphyrin–C<sub>60</sub> film show decreased porphyrin C1s and N1s binding energies relative to uncomplexed porphyrin.<sup>33</sup> This has been interpreted in terms of charge transfer from the fullerene to the metalloporphyrin.

Understanding the nature of the fullerene–porphyrin interaction has two components. Primarily, the attractive interaction is driven by the dispersive forces associated with  $\pi$ – $\pi$  interactions. This is most straightforwardly illustrated by the side-on rather than end-on binding of C<sub>70</sub>. The close approaches observed in cocrystallates and host–guest complexes, including the relative orientations of bonds, can be well reproduced using empirical molecular mechanics modeling the force fields of which include van der Waals terms.<sup>6,14,34</sup> Semiempirical and minimal basis set ab initio calculations do not reproduce the close approach. This is an expected result if van der Waals interactions are dominant because these calculations do not take into account electron correlation.

The experimental data summarized above support the idea that the fundamentally strong  $\pi$ – $\pi$  interaction is augmented by weak electrostatic or covalent donor–acceptor stabilization. The frequently observed alignment of a fullerene 6:6 ring juncture “double” bond with a trans N···N vector (Figure 8) has been rationalized on electrostatic grounds.<sup>37</sup> The electron-rich porphyrin N atoms are positioned over regions of positive electrostatic potential near the centers of the fullerene rings. This is consistent with the prevailing view of porphyrin dimers where dispersion forces create the fundamental attraction and weaker electrostatic forces control the mutual orientation.<sup>3</sup>

More controversial is the concept of the fullerene acting as a donor to the porphyrin or metalloporphyrin. Until

**FIGURE 8.** Orientation of the 6:6 ring juncture of C<sub>60</sub> (green) over the porphyrin plane (black) showing near alignment with a trans N···N vector.

the discovery of fullerene–porphyrin complexation, fullerenes were known chiefly for their electron-acceptor properties. For example, C<sub>60</sub> readily forms C<sub>60</sub><sup>n−</sup> fullerides,<sup>35</sup> and fullerenes are the acceptors in fullerene–porphyrin conjugate photochemistry.<sup>36</sup> We proposed that the higher electron density in the “double” bond at the 6:6 ring juncture of C<sub>60</sub> or C<sub>70</sub> was attracted to the protic center of a free-base porphyrin or the electropositive center of a metalloporphyrin.<sup>2</sup> Recent NEXAFS experiments support the idea that the 6:6 ring juncture bond can donate electron density to the porphyrin or metalloporphyrin, but density functional calculations using a Voronoi deformation density analysis come to the opposite conclusion.<sup>37</sup> At a global level, fullerenes are expected to be electron acceptors in a charge-transfer complex, but at the local level, a specific fullerene bond may donate electron density to the positive center of a porphyrin or metalloporphyrin.

The difficulty of defining the energetics of the interaction and the direction of overall electron flow arise from the relatively small magnitudes of the electrostatic and covalent components. As a consequence, it has not been easy to rationalize the binding constants of fullerenes in a series of metalloporphyrin hosts (Table 1). It is clear that a number of small effects conspire to affect binding constants in ways that do not always lend themselves to easy deconvolution. The report<sup>19</sup> that the order of binding constants changes slightly between C<sub>60</sub> and C<sub>70</sub> for the same host shows that subtle differences in solvation energies are another factor.<sup>14</sup>

The enthalpy of the fullerene–porphyrin interaction has been determined from retention times in variable temperature chromatographic studies using Zn(TPP)-appended silica gel stationary phases.<sup>38</sup> In toluene, the “enthalpy of transfer” is  $1.5 \text{ kcal}\cdot\text{mol}^{-1}$  for C<sub>60</sub> and  $2.4 \text{ kcal}\cdot\text{mol}^{-1}$  for C<sub>70</sub>. These small values reflect the high energetic cost of displacing arene solvent from around

both the fullerene and the porphyrin. “Gas phase” estimates of the binding enthalpy have been made using density functional calculations<sup>6,37,39</sup> and usually give much larger values, but DFT is well-known to show erratic performance in the calculation of van der Waals interactions.<sup>40</sup> Relating calculated values to experimental determinations will require solvation to be taken into account.

## Chromatographic Applications

Prior to the structural observation of discrete fullerene–porphyrin complexes, the fullerene–porphyrin interaction had been proposed as the basis for selectivity in fullerene chromatography using zinc porphyrin-appended silica stationary phases.<sup>41</sup> Long retention times are associated with larger-sized fullerenes, consistent with greater  $\pi$ – $\pi$  contact areas. A parallel is seen in the selectivity for  $C_{70}$  over  $C_{60}$  observed in static solution with “Jaws” porphyrins.<sup>14</sup> Columns of porphyrin-appended silica are also superior for the separation of endohedral metallofullerenes such as  $\text{Ln}@C_{82}$ .<sup>41</sup> Their longer retention times relative to isostructural metal-free fullerenes are consistent with the idea that endohedral fullerenes have external fulleride character, arising from the positive oxidation state of the metal and are therefore better donors to a metalloporphyrin. Again, a parallel is seen in the stronger binding of  $\text{Gd}@C_{82}$  relative to  $C_{82}$  with “Jaws” porphyrin in mass spectrometric measurements.<sup>14</sup> Very recently, cyclic porphyrin dimers have been shown to selectively extract higher fullerenes.<sup>42</sup>

## Fullerene-Pillared Metalloporphyrin Frameworks

The tetragonal shapes of porphyrins and the globular shapes of fullerenes make them attractive candidates for assembling extended supramolecular framework solids.<sup>43</sup> We wondered whether the fullerene–porphyrin interaction was sufficiently strong to act as a structure-defining element with layered porphyrinic structures. Interleaved fullerene “pillars” might strengthen porous porphyrin frameworks giving them greater potential as zeolite analogues.

When tetra(4-pyridylporphyrin) ( $\text{H}_2\text{TpyP}$ ) is treated with  $\text{Pb}^{\text{II}}$  halides, a 2D infinite sheet structure is formed.<sup>44</sup> A portion of this layer is shown in Figure 9. As shown in Figure 10, a layer of solvent molecules is sandwiched between the porphyrin sheets the interlayer separation of which is 5.5 Å. The porphyrins are not in strict perpendicular alignment. Rather, they are offset (or slipped) from each other by 10.5 Å.

When  $C_{60}$  is included in the crystallizing mixture of  $\text{H}_2\text{TpyP}$  and  $\text{Pb}(\text{NO}_3)_2$ , the fullerene intercalates into the solvent layer producing a fullerene-pillared structure.<sup>8</sup> As illustrated in Figure 11, the fullerenes are sandwiched between porphyrinic layers. The interlayer separation has increased to 12.1 Å, accommodating the 10 Å van der Waals diameter of  $C_{60}$  plus some tetrachloroethane solvate molecules. As expected for a supramolecular association, there are no significant changes in the bond distances and

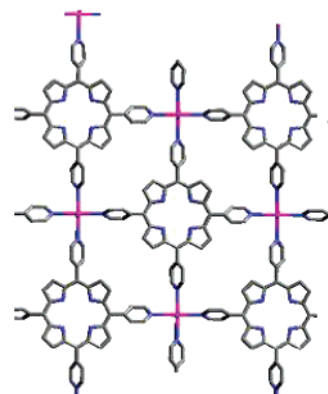


**FIGURE 9.** Sheet structure of  $\text{H}_2\text{TpyP}\cdot\text{Pb}^{2+}$  layers in  $\text{H}_2\text{TpyP}\cdot\text{PbI}_2\cdot 4\text{C}_2\text{H}_2\text{Cl}_4$ .<sup>44</sup> Iodide ligands lie directly above and below the Pb atoms (magenta).

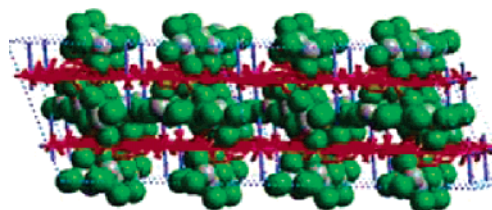


**FIGURE 10.** Alternating solvent (green) and porphyrin (red) layers in  $\text{H}_2\text{TpyP}\cdot\text{PbI}_2\cdot 4\text{C}_2\text{H}_2\text{Cl}_4$ .<sup>44</sup>

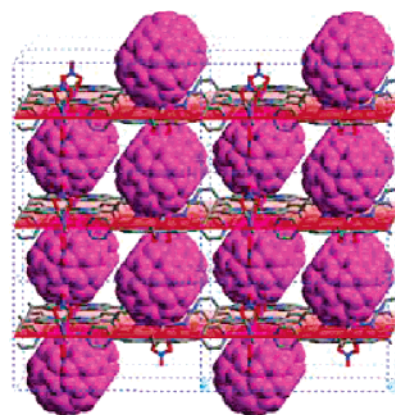


**FIGURE 11.** Alternating  $C_{60}$  (magenta) and porphyrin (red) layers in  $\text{H}_2\text{TpyP}\cdot\text{C}_{60}\cdot\text{Pb}(\text{NO}_3)_2\cdot 1.5\text{TCE}$ .<sup>8</sup> Solvent molecules have been omitted for clarity.

angles of the components relative to those found in unassociated fullerene and porphyrin structures. The shortest approach of a fullerene C atom to the porphyrin plane is 2.59 Å, the shortest yet observed for a free-base porphyrin–fullerene interaction. As in discrete molecule porphyrin–fullerene cocrystallates, a 6:6 ring juncture bond of the fullerene is closest to the porphyrin and is precisely aligned with a trans  $\text{N}\cdots\text{N}$  vector of the porphyrin. Notably, the alignment of the porphyrins shows strict tetragonal register. There is no vertical offset (or slippage). This is taken as evidence that the fullerene–porphyrin supramolecular interaction is a truly structure-defining element. Disordered tetrachloroethane solvent molecules partially fill the voids in the lattice. The free volume in the structure for solvent is remarkably high: ca. 52%. This was estimated from the cavities left after the van der Waals

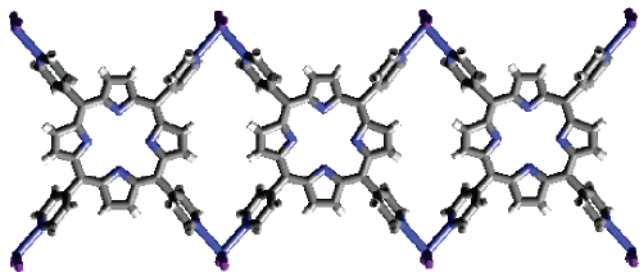


**FIGURE 12.** Plan view of the ribbon structure of  $\text{H}_2\text{TpyP}\cdot 2\text{HgI}_2\cdot \text{C}_{70}\cdot \text{solvent}$ .<sup>8</sup>

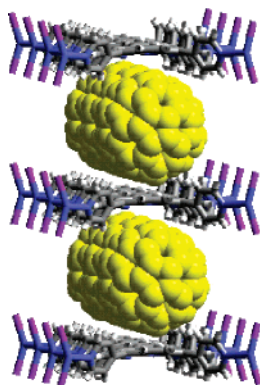


**FIGURE 13.** Perspective view along the ribbon direction in  $\text{H}_2\text{TpyP}\cdot 2\text{HgI}_2\cdot \text{C}_{70}\cdot \text{solvent}$ .<sup>8</sup>

surfaces are generated for the porphyrin–fullerene assembly. There are channels along the 4-fold axis and the zigzag spaces perpendicular to the 4-fold axis between the fullerenes.

A similar cocrystallization of  $\text{Pb}(\text{NO}_3)_2$ ,  $\text{H}_2\text{TpyP}$ , and the larger, egg-shaped fullerene  $\text{C}_{70}$  also leads to an intercalated material with strict tetragonal register and an interlayer separation of 12.5 Å.<sup>8</sup> This is consistent with side-on rather than end-on binding of the  $\text{C}_{70}$  pillars, maximizing van der Waals interactions.

A closely related cocrystallization of  $\text{H}_2\text{TpyP}$  and  $\text{C}_{70}$  with mercuric iodide instead of lead nitrate yields a structure containing porphyrin ribbons rather than sheets.<sup>8</sup> The porphyrin ribbon motif, shown in Figure 12, is very similar to that found in the non-fullerene-containing structure of  $\text{H}_2\text{TpyP}\cdot 2\text{HgBr}_2\cdot 2\text{CHCl}_3$ .<sup>45</sup> As in the sheet structures, the fullerenes bring the porphyrins into perpendicular register and pry the ribbons ca. 12.5 Å apart. This accommodates  $\text{C}_{70}$  in a side-on orientation with its 5-fold axis along the direction of the ribbon. This is shown in Figure 13. The ribbons are interleaved leaving less free space for solvent than in the sheet structure, 30% compared to 52%.

There is wide interest in the idea that porous channels in porphyrin framework solids can act as zeolite analogues in separations, catalysis, and sensor applications.<sup>46</sup> Most porphyrin framework structures collapse irreversibly upon total removal of solvent molecules, and this fragility has slowed progress toward functional materials. However, the recent success by Suslick and co-workers<sup>47,48</sup> in demonstrating reversible size- and shape-selective adsorption/desorption and desiccant properties with a cobalt-linked carboxylate porphyrin (PIZA-1) encourages further explo-

ration. Preliminary experiments<sup>8</sup> with the layered sheet compound  $\text{H}_2\text{TpyP}\cdot \text{C}_{60}\cdot \text{Pb}(\text{NO}_3)_2\cdot 1.5\text{TCE}$  suggest that the fullerene pillars do indeed add strength to the framework structure. As judged by thermogravimetric analysis and elemental composition with energy-dispersive X-ray microanalysis under scanning electron microscopy conditions, approximately 80% of the solvent can be removed by heating to 250 °C under vacuum for 2 days. The powder XRD pattern changes as a result of this treatment, but there is no significant diminution of crystallinity. These features parallel the behavior reported for PIZA-1.

## Nanostructure Applications

In addition to the application of fullerene-pillared frameworks as possible zeolite analogues, the idea that the fullerene–porphyrin recognition element can be used as an organizing force to produce nanoscale particles has also been pursued.

Derivatized fullerenes are well-known to aggregate into a variety of nanoscale rods and vesicles. When the derivatization includes an appended porphyrin on  $\text{C}_{60}$ , 30–500 nm tubules assemble from aqueous solution under sonication.<sup>49</sup> Whether this aggregation is driven by porphyrin–porphyrin attraction or porphyrin–fullerene attraction has not been experimentally determined, but calculations favor the former. On the other hand, in dendritically elaborated porphyrins, there is good NMR and UV–vis evidence that fullerenes bind in the cleft of acyclic bisporphyrins, driving the formation of peapod-like tubules.<sup>50</sup> An oriented adlayer of a fullerene derivative has been prepared on a gold electrode by first depositing  $\text{Zn}(\text{OEP})$ .<sup>51</sup>

Kamat and co-workers have exploited fullerene–porphyrin aggregation to form stable clusters of 5,15-bis(3,5-*tert*-butylphenyl)porphyrin and  $\text{C}_{60}$  in acetonitrile–toluene solutions.<sup>52</sup> New broad and intense absorptions appear in the visible and NIR spectral regions relative to fullerene clusters or porphyrin clusters suggesting a charge-transfer interaction between the two different chromophores. The clusters can be transferred onto a  $\text{SnO}_2$  surface to form particles of 200–300 nm size or allowed to crystallize into well-defined microcrystallites. These presumably have the same kinds of structures as seen earlier in single crystals derived from traditional cocrystallization techniques. The surface-absorbed clusters show enhanced light-harvesting characteristics that are significantly better than the additive effect observed from either porphyrin or fullerene clusters. The incident photon-to-photocurrent efficiency is 17% for the composite but only 1.6% for the porphyrin-only cluster and 5% for the fullerene-only cluster. This increased efficiency in electron/hole separation must arise from the organizational elements of the supramolecular fullerene–porphyrin cluster.

## Conclusions

The spontaneous attraction of a fullerene to the center of a porphyrin is a new structure-defining supramolecular recognition element that can be used to produce discrete

host–guest complexes, extended porous framework solids, and nanoscale particles. The interaction is essentially van der Waals in nature but is perturbed by weak electrostatic and possible charge-transfer effects. It has been central to the success of the chromatographic separation of higher fullerenes and endohedral fullerenes in porphyrin-appended silica gel stationary phases, and there are promising indications of useful applications in the areas of zeolite analogues and photovoltaic devices.

*This work has been supported by the Marsden Fund of the Royal Society of New Zealand (Grant 00-UOA-15) and the National Institutes of Health (Grant GM 23851).*

## References

- Balch, A. L.; Olmstead, M. M. Structural Chemistry of Supramolecular Assemblies that Place Flat Molecular Surfaces Around the Curved Exteriors of Fullerenes. *Coord. Chem. Rev.* **1999**, *185–186*, 601–617.
- Sun, Y.; Drovetskaya, T.; Bolskar, R. D.; Bau, R.; Boyd, P. D. W.; Reed, C. A. Fullerides of Pyrrolidine-Functionalized C<sub>60</sub>. *J. Org. Chem.* **1997**, *62*, 3642–3649.
- Hunter, C. A. Meldola Lecture – the Role of Aromatic Interactions in Molecular Recognition. *Chem. Soc. Rev.* **1994**, *23*, 101–109.
- Scheidt, W. R.; Lee, Y. J. In *Structure and Bonding*; Springer-Verlag: Berlin, 1987; Vol. 64; pp 1–70.
- Eichhorn, D. M.; Yang, S.; Jarrell, W.; Baumann, T. F.; Beall, L. S.; White, A. J. P.; Williams, D. J.; Barrett, A. G. M.; Hoffman, B. M. [60]Fullerene and TCNQ Donor–Acceptor Crystals of Octakis(dimethylamino)porphyrazine. *J. Chem. Soc., Chem. Commun.* **1995**, 1703–1704.
- Boyd, P. D. W.; Hodgson, M. C.; Chaker, L.; Rickard, C. E. F.; Oliver, A. G.; Brothers, P. J.; Bolskar, R.; Tham, F. S.; Reed, C. A. Selective Supramolecular Fullerene–Porphyrin Interactions. *J. Am. Chem. Soc.* **1999**, *121*, 10487–10495.
- Olmstead, M. M.; Costa, D. A.; Maitra, K.; Noll, B. C.; Phillips, S. L.; Van Calcar, P. M.; Balch, A. L. Interaction of Curved and Flat Molecular Surfaces. The Structures of Crystalline Compounds Composed of Fullerene (C<sub>60</sub>, C<sub>60</sub>O, C<sub>70</sub>, and C<sub>120</sub>O) and Metal Octaethylporphyrin Units. *J. Am. Chem. Soc.* **1999**, *121*, 7090–7097.
- Sun, D.; Tham, F. S.; Reed, C. A.; Boyd, P. D. W. Extending Supramolecular Fullerene–Porphyrin Chemistry to Metal–Organic Frameworks. *Proc. Natl. Acad. Sci. U.S.A.* **2002**, *99*, 5088–5092 and references therein.
- Olmstead, M. M.; Lee, H. M.; Duchamp, J. C.; Stevenson, S.; Marcu, D.; Dorn, H. C.; Balch, A. L. Sc<sub>3</sub>N@C<sub>68</sub>: Folded pentalene coordination in an endohedral fullerene that does not obey the isolated pentagon rule. *Angew. Chem., Int. Ed.* **2003**, *42*, 900–903 and references therein.
- Hochmuth, D. H.; Michel, S. L. J.; White, A. J. P.; Williams, D. J.; Barrett, A. G. M.; Hoffman, B. M. C<sub>2</sub> Symmetric and Non-Centrosymmetric Crystalline Complexes of [60]Fullerene with Octakis(dimethylamino)porphyrinato-Copper(II) and -Nickel(II). *Eur. J. Inorg. Chem.* **2000**, 593–596.
- Ishii, T.; Aizawa, N.; Yamashita, M.; Matsuzaka, H.; Kodama, T.; Kikuchi, K.; Ikemoto, I.; Iwasa, Y. First Syntheses of Cocrystallites Consisting of *anti*-Formed Metal Octaethylporphyrins with Fullerene C<sub>60</sub>. *J. Chem. Soc., Dalton Trans.* **2000**, 4407–4412.
- Konarev, D. V.; Neretin, I. S.; Slovokhotov, Y. L.; Yudanov, E. I.; Drichko, N. V.; Shul'ga, Y. M.; Tarasov, B. P.; Gumanov, K. L.; Batsanov, A. S.; Howard, J. A. K.; Lyubovskaya, R. N. New Molecular Complexes of Fullerenes C<sub>60</sub> and C<sub>70</sub> with Tetraphenylporphyrins [M(tp)], in which M = H<sub>2</sub>, Mn, Co, Cu, Zn, and FeCl. *Chem.–Eur. J.* **2001**, *7*, 2605–2616.
- Ishii, T.; Aizawa, N.; Kanehama, R.; Yamashita, M.; Sugiura, K. I.; Miyasaka, H. Cocrystallites consisting of metal macrocycles with fullerenes. *Coord. Chem. Rev.* **2002**, *226*, 113–124.
- Sun, D. Y.; Tham, F. S.; Reed, C. A.; Chaker, L.; Boyd, P. D. W. Supramolecular fullerene–porphyrin chemistry. Fullerene complexation by metalated “jaws porphyrin” hosts. *J. Am. Chem. Soc.* **2002**, *124*, 6604–6612.
- Stöhr, M.; Wagner, T.; Gabriel, M.; Weyers, B.; Möller, R. Direct observation of hindered eccentric rotation of an individual molecule: Cu-phthalocyanine on C<sub>60</sub>. *Phys. Rev. B* **2002**, *65*, 033404.
- de Wild, M.; Berner, S.; Suzuki, H.; Yanagi, H.; Schlettwein, D.; Ivan, S.; Baratoff, A.; Guentherodt, H. J.; Jung, T. A. A novel route to molecular self-assembly: Self-intermixed monolayer phases. *ChemPhysChem* **2002**, *3*, 881–885.
- Hosseini, A.; Boyd, P. D. W.; Tham, F. S.; Reed, C. A. Unpublished results.
- Tashiro, K.; Aida, T.; Zheng, J.-Y.; Kinbara, K.; Saigo, K.; Sakamoto, S.; Yamaguchi, K. A Cyclic Dimer of Metalloporphyrin Forms a Highly Stable Inclusion Complex with C<sub>60</sub>. *J. Am. Chem. Soc.* **1999**, *121*, 9477–9478.
- Zheng, J.-Y.; Tashiro, K.; Hirabayashi, Y.; Kinbara, K.; Saigo, K.; Aida, T.; Sakamoto, S.; Yamaguchi, K. Cyclic Dimers of Metalloporphyrins as Tunable Hosts for Fullerenes: A Remarkable Effect of Rhodium(III). *Angew. Chem., Int. Ed.* **2001**, *40*, 1858–1861.
- Sun, D.; Tham, F. S.; Reed, C. A.; Chaker, L.; Burgess, M.; Boyd, P. D. W. Porphyrin–Fullerene Host–Guest Chemistry. *J. Am. Chem. Soc.* **2000**, *122*, 10704–10705.
- Ayabe, M.; Ikeda, A.; Shinkai, S.; Sakamoto, S.; Yamaguchi, K. A novel [60]fullerene receptor with a Pd(II)-switched bisporphyrin cleft. *Chem. Commun.* **2002**, *10*, 1032–1033.
- Ayabe, M.; Ikeda, A.; Kubo, Y.; Takeuchi, M.; Shinkai, S. A Dendritic Porphyrin Receptor for C<sub>60</sub> Which Features a Profound Positive Allosteric Effect. *Angew. Chem., Int. Ed.* **2002**, *41*, 2790–2792.
- Kubo, Y.; Sugasaki, A.; Ikeda, M.; Sugiyasu, K.; Sonoda, K.; Ikeda, A.; Takeuchi, M.; Shinkai, S. Cooperative C<sub>60</sub> Binding to a Porphyrin Tetramer Arranged around a p-Terphenyl Axis in 1:2 Host–Guest Stoichiometry. *Org. Lett.* **2002**, *4*, 925–928.
- Dudic, M.; Lhoták, P.; Stibor, I.; Petřícková, H.; Lang, K. (Thia)calix 4 arene-porphyrin conjugates: novel receptors for fullerene complexation with C<sub>70</sub> over C<sub>60</sub> selectivity. *New. J. Chem.* **2004**, *28*, 85–90.
- Kimura, M.; Saito, Y.; Ohta, K.; Hanabusa, K.; Shirai, H.; Kobayashi, N. Self-Organization of Supramolecular Complex Composed of Rigid Dendritic Porphyrin and Fullerene. *J. Am. Chem. Soc.* **2002**, *124*, 5274–5275.
- Guldi, D. M.; Da Ros, T.; Braiucă, P.; Prato, M.; Alessio, E. C<sub>60</sub> in the box. A supramolecular C<sub>60</sub>-porphyrin assembly. *J. Mater. Chem.* **2002**, *12*, 2001–2008.
- Shirakawa, M.; Fujita, N.; Shinkai, S. [60]Fullerene-Motivated Organogel Formation in a Porphyrin Derivative Bearing Programmed Hydrogen-Bonding Sites. *J. Am. Chem. Soc.* **2003**, *125*, 9902–9903.
- Solladie, N.; Walther, M. E.; Gross, M.; Duarte, T. M. F.; Bourgonne, C.; Nierengarten, J. F. A supramolecular cup-and-ball C<sub>60</sub>-porphyrin conjugate system. *Chem. Commun.* **2003**, 2412–2413.
- Tashiro, K.; Hirabayashi, Y.; Aida, T.; Saigo, K.; Fujiwara, K.; Komatsu, K.; Sakamoto, S.; Yamaguchi, K. A supramolecular oscillator composed of carbon nanocluster C<sub>120</sub> and a rhodium(III) porphyrin cyclic dimer. *J. Am. Chem. Soc.* **2002**, *124*, 12086–12087.
- Evans, D. R.; Fackler, N. L. P.; Xie, Z.; Rickard, C. E. F.; Boyd, P. D. W.; Reed, C. A. π-Arene/Cation Structure and Bonding. Solvation versus Ligand Binding in Iron(III) Tetraphenylporphyrin Complexes of Benzene, Toluene, p-Xylene, and [60]Fullerene. *J. Am. Chem. Soc.* **1999**, *121*, 8466–8474.
- Konarev, D. V.; Khasanov, S. S.; Saito, G.; Lyubovskaya, R. N.; Yoshida, Y.; Otsuka, A. The Interaction of C<sub>60</sub>, C<sub>70</sub>, and C<sub>60</sub>(CN)<sub>2</sub> Radical Anions with Cobalt(II) Tetraphenylporphyrin in Solid Multicomponent Complexes. *Chem.–Eur. J.* **2003**, *9*, 3837–3848.
- Tkachenko, N. V.; Guenther, C.; Imahori, H.; Tamaki, K.; Sakata, Y.; Fukuzumi, S.; Lemmetyinen, H. Near infrared emission of charge-transfer complexes of porphyrin–fullerene films. *Chem. Phys. Lett.* **2000**, *326*, 344–350.
- Polzonetti, G.; Battocchio, C.; Goldoni, A.; Larciprete, R.; Caravatta, V.; Paolesso, R.; Russo, M. V. Interface formation between C<sub>60</sub> and diethynyl-Zn-porphyrinato investigated by SR-induced photoelectron and near-edge X-ray absorption (NEXAFS) spectroscopies. *Chem. Phys.* **2004**, *297*, 307–314.
- Schuster, D. I.; Jarowski, P. D.; Kirschner, A. N.; Wilson, S. R. Molecular modelling of fullerene-porphyrin dyads. *J. Mater. Chem.* **2002**, *12*, 2041–2047.
- Reed, C. A.; Bolskar, R. D. Discrete Fulleride Anions and Fullerenium Cations. *Chem. Rev.* **2000**, *100*, 1075–1119.
- Guldi, D. M. Fullerenes: Three-Dimensional Electron Acceptor Materials. *Chem. Commun.* **2000**, 321–327.
- Wang, Y. B.; Lin, Z. Y. Supramolecular Interactions between Fullerenes and Porphyrins. *J. Am. Chem. Soc.* **2003**, *125*, 6072–6073.
- Xiao, J.; Meyerhoff, M. E. High-Performance Liquid-Chromatography of C<sub>60</sub>, C<sub>70</sub>, and Higher Fullerenes on Tetraphenylporphyrin-



- Silica Stationary Phases Using Strong Mobile-Phase Solvents. *J. Chromatogr. A* **1995**, *715*, 19–29.
- (39) Shephard, M. J.; Paddon-Row, M. N. The porphyrin- $C_{60}$  non-bonded interaction: an ab initio MO and DFT study. *J. Porphyrins Phthalocyanines* **2002**, *6*, 783–794.
- (40) Xu, X.; Goddard, W. A. The X3LYP extended density functional for accurate descriptions of nonbond interactions, spin states, and thermochemical properties. *Proc. Natl. Acad. Sci. U.S.A.* **2004**, *101*, 2673–2677.
- (41) Xiao, J.; Savina, M. R.; Martin, G. B.; Francis, A. H.; Meyerhoff, M. E. Efficient HPLC Purification of Endohedral Metallofullerenes on a Porphyrin-Silica Stationary Phase. *J. Am. Chem. Soc.* **1994**, *116*, 9341–9342.
- (42) Shoji, Y.; Tashiro, K.; Aida, T. Selective Extraction of Higher Fullerenes Using Cyclic Dimers of Zinc Porphyrins. *J. Am. Chem. Soc.* **2004**, *126*, 6570–6571.
- (43) Abrahams, B. F.; Hoskins, B. F.; Michail, D. M.; Robson, R. Assembly of porphyrin building blocks into network structures with large channels. *Nature* **1994**, *369*, 727–729.
- (44) Sharma, C. V. K.; Broker, G. A.; Huddleston, J. G.; Baldwin, J. W.; Metzger, R. M.; Rogers, R. D. Design Strategies for Solid-State Supramolecular Arrays Containing Both Mixed-Metalated and Freebase Porphyrins. *J. Am. Chem. Soc.* **1999**, *121*, 1137–1144.
- (45) Pan, L.; Noll, B. C.; Wang, X. Self-Assembly of Free-Base Tetrapyrrolylporphyrin Units by Metal Ion Coordination. *Chem. Commun.* **1999**, 157–158.
- (46) Kosal, M. E.; Suslick, K. S. Microporous porphyrin and metalloporphyrin materials. *J. Solid State Chem.* **2000**, *152*, 87–98.
- (47) Kosal, M. E.; Chou, J. H.; Wilson, S. R.; Suslick, K. S. A functional zeolite analogue assembled from metalloporphyrins. *Nat. Mater.* **2002**, *1*, 118–121.
- (48) Suslick, K. S.; Bhyrappa, P.; Chou, J.-H.; Kosal, M. E.; Nakagaki, S.; Smithenry, D. W.; Wilson, S. R. Microporous Porphyrin Solids. *Acc. Chem. Res.*, in press.
- (49) Georgakilas, V.; Pellarini, F.; Prato, M.; Guldi, D. M.; Melle-Franco, M.; Zerbetto, F. Supramolecular self-assembled fullerene nanostructures. *Proc. Natl. Acad. Sci. U.S.A.* **2002**, *99*, 5075–5080.
- (50) Yamaguchi, T.; Ishii, N.; Tashiro, K.; Aida, T. Supramolecular Peapods Composed of a Metalloporphyrin Nanotube and Fullerenes. *J. Am. Chem. Soc.* **2003**, *125*, 13934–13935.
- (51) Yoshimoto, S.; Tsutsumi, E.; Honda, Y.; Murata, Y.; Murata, M.; Komatsu, K.; Ito, O.; Itaya, K. Controlled Molecular Orientation in an Adlayer of a Supramolecular Assembly Consisting of an Open-Cage  $C_{60}$  Derivative and  $Zn^{II}$  Octaethylporphyrin on Au(111). *Angew. Chem., Int. Ed.* **2004**, *43*, 3044–3047.
- (52) Hasobe, T.; Imahori, H.; Fukuzumi, S.; Kamat, P. V. Light Energy Conversion Using Mixed Molecular Nanoclusters. Porphyrin and  $C_{60}$  Cluster Films for Efficient Photocurrent Generation. *J. Phys. Chem. B* **2003**, *107*, 12105–12112.

AR040168F